Interplay between Topology and Edge Weights in Real-World Graphs: Online Appendix

1 Full results w.r.t the observations

1.1 Observation 1: adjacency and weightiness

In Figures 1 to 11, for each dataset and each $1 \leq i \leq 5$, we report how (a) the fraction of adjacent pairs within each group of pairs (i.e., $|E_{c;i}|/|R_{c;i}|$) and (b) the fraction of weighty edges within each group of edges (i.e., $f_{c;i}$) depend on the number of CNs, and include the Pearson correlation coefficient between the two sequences.
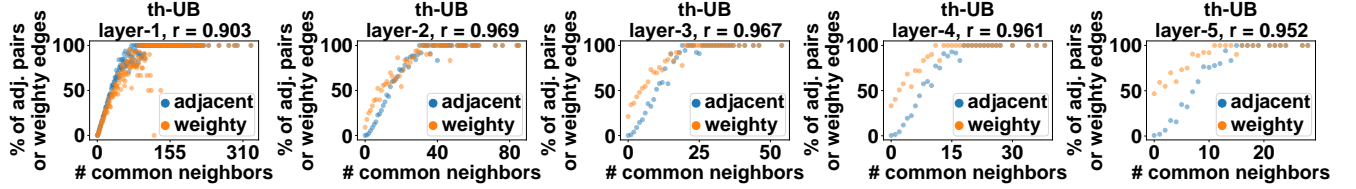

Figure 1: The full results w.r.t Observation 1 on *th-UB*.
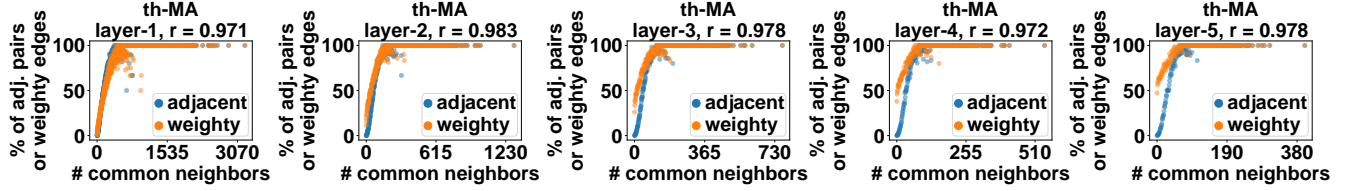

Figure 2: The full results w.r.t Observation 1 on *th-MA*.
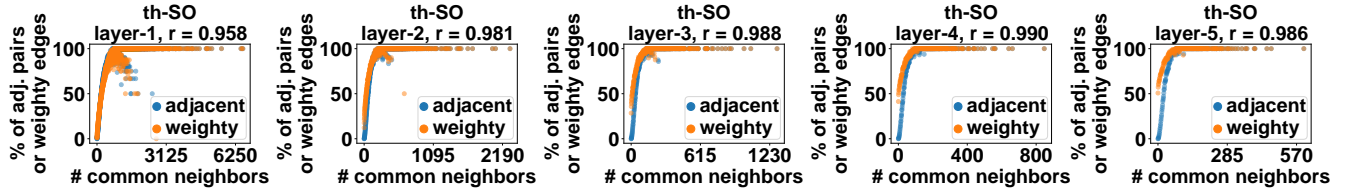

Figure 3: The full results w.r.t Observation 1 on *th-SO*.
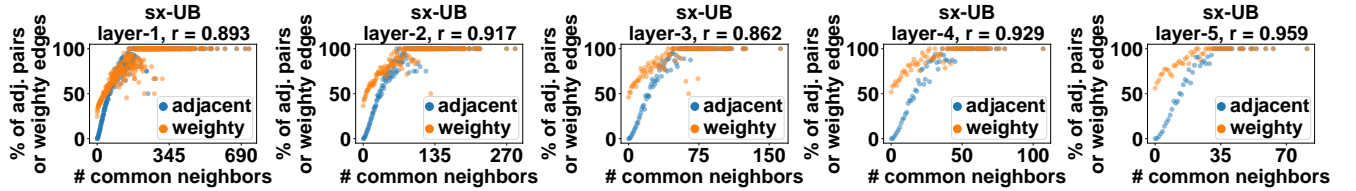

Figure 4: The full results w.r.t Observation 1 on *sx-UB*.
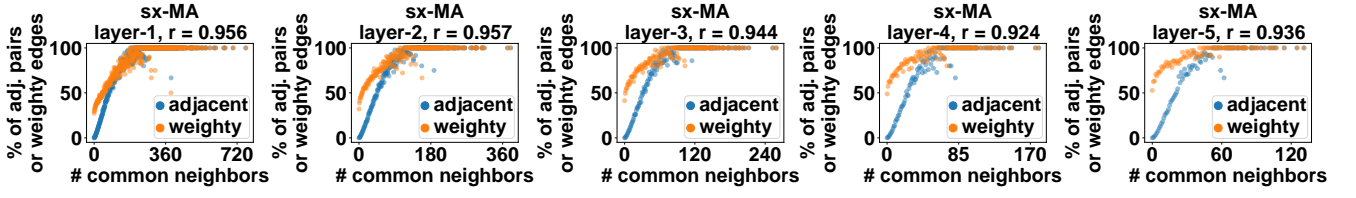
Figure 5: The full results w.r.t Observation 1 on *sx-MA*.
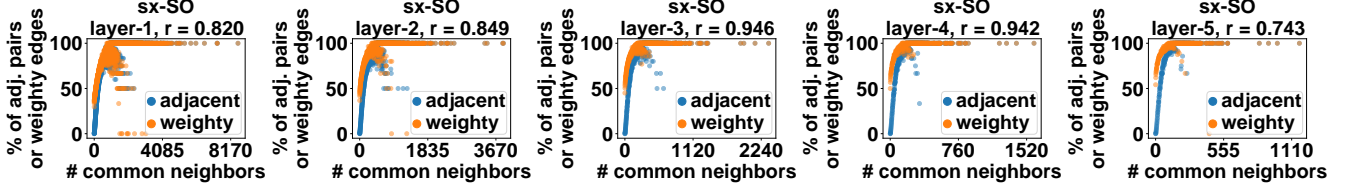

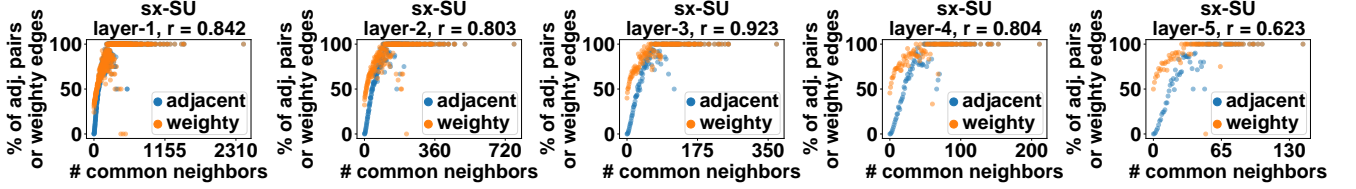Figure 6: The full results w.r.t Observation 1 on *sx-SO*.

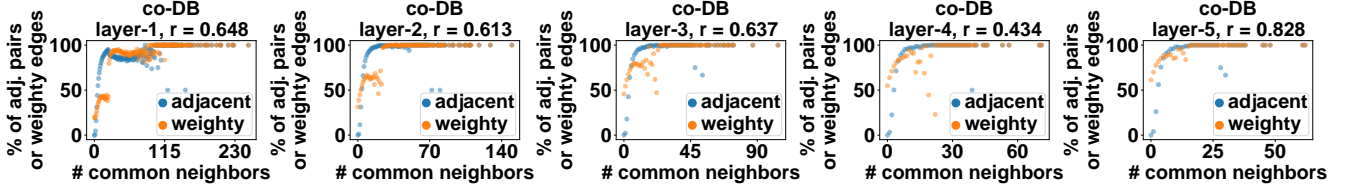Figure 7: The full results w.r.t Observation 1 on *sx-SU*.

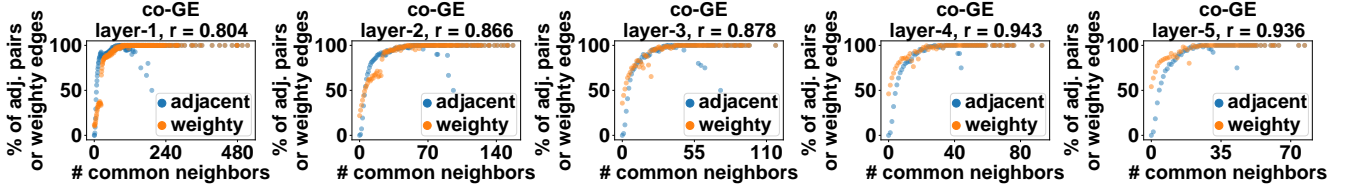Figure 8: The full results w.r.t Observation 1 on *co-DB*.

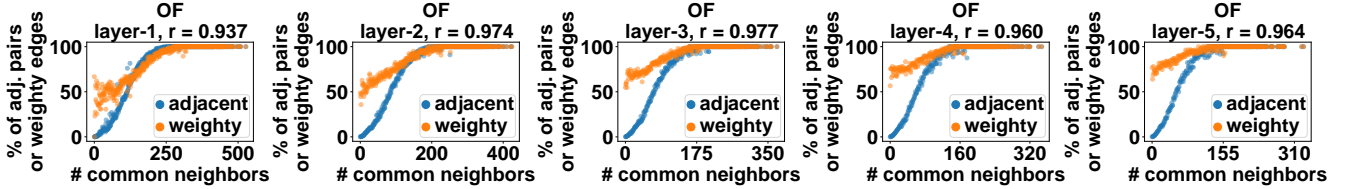Figure 9: The full results w.r.t Observation 1 on *co-GE*.

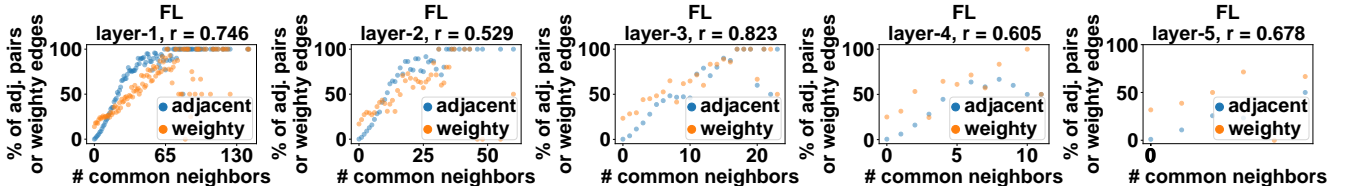Figure 10: The full results w.r.t Observation 1 on *OF*.

Figure 11: The full results w.r.t Observation 1 on *FL*.

2

1.2 Observation 2: the fractions of weighty edges

In Figures 12 to 22, for each dataset and each $1 \leq i \leq 5$, we plot the fractions of weighty edges (FoWEs) with the results of the linear fitting for the points truncated before the saturation point, and include the R^2 value of the linear fitting.
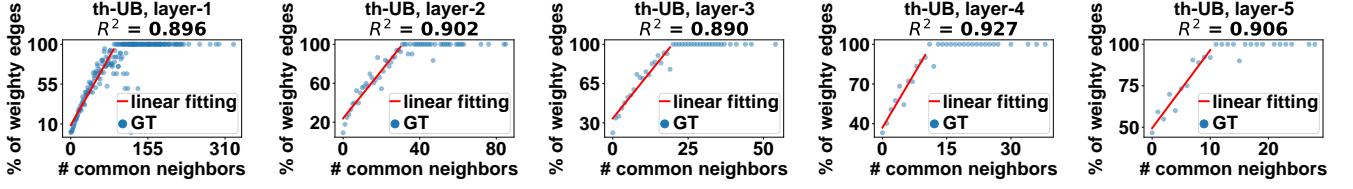

Figure 12: The full results w.r.t Observation 2 on *th-UB*.
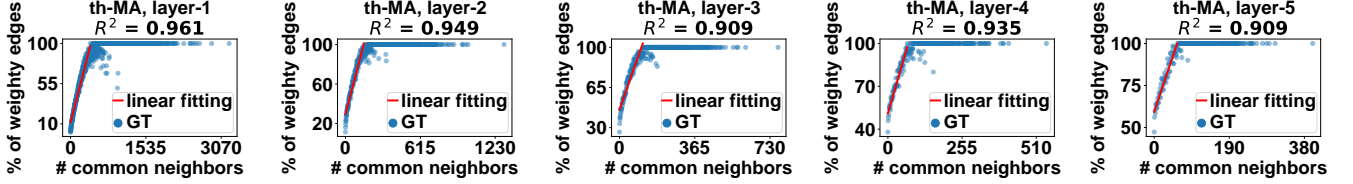

Figure 13: The full results w.r.t Observation 2 on *th-MA*.
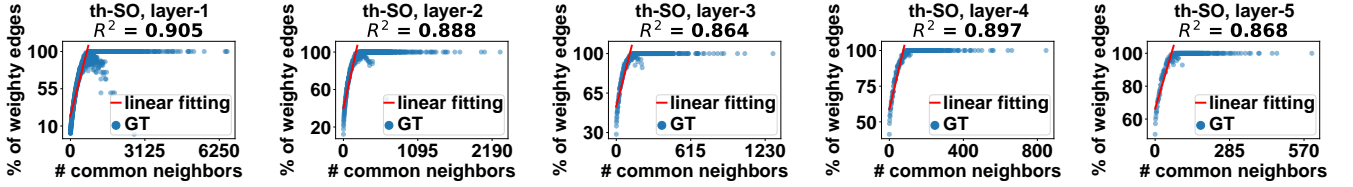

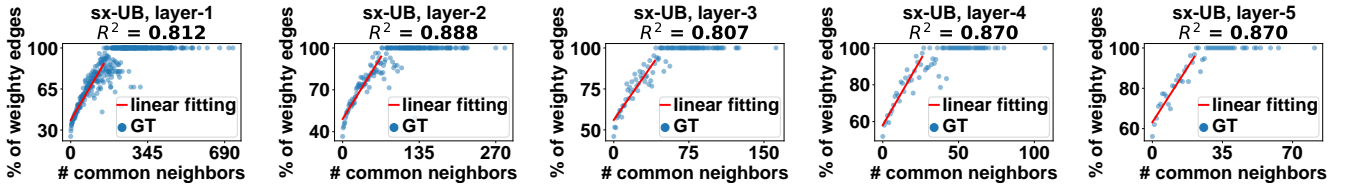Figure 14: The full results w.r.t Observation 2 on *th-SO*.

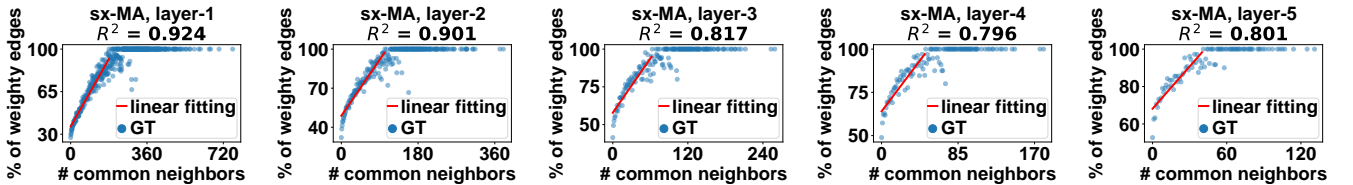Figure 15: The full results w.r.t Observation 2 on *sx-UB*.

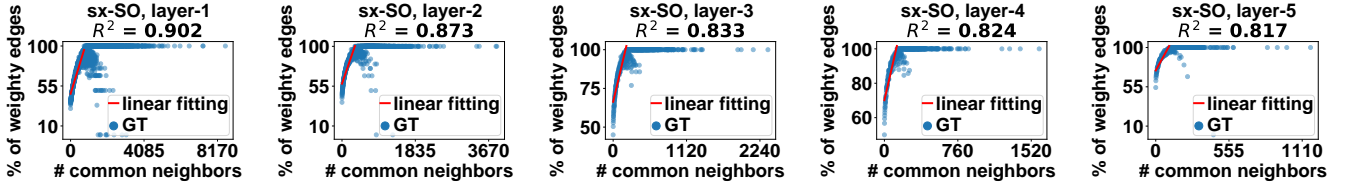Figure 16: The full results w.r.t Observation 2 on *sx-MA*.

3

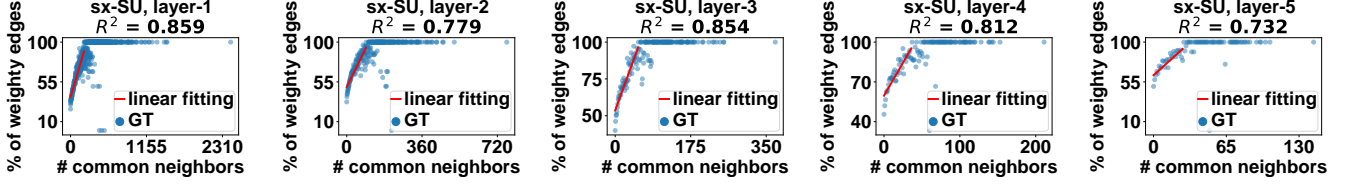Figure 17: The full results w.r.t Observation 2 on *sx-SO*.

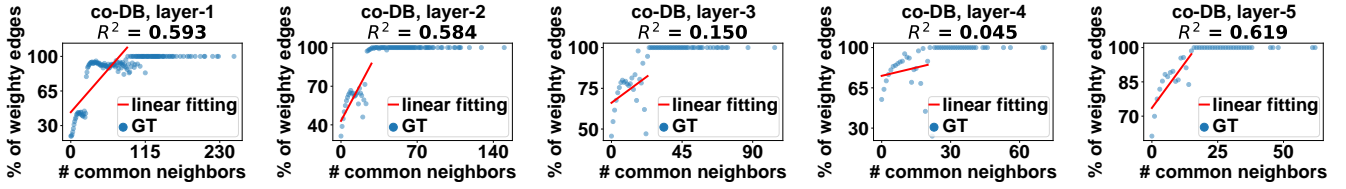Figure 18: The full results w.r.t Observation 2 on *sx-SU*.

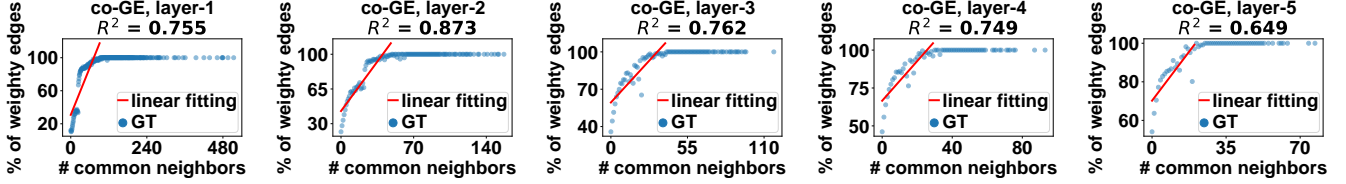Figure 19: The full results w.r.t Observation 2 on *co-DB*.

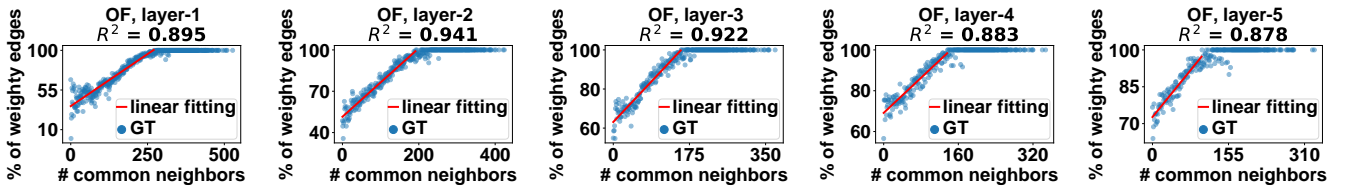Figure 20: The full results w.r.t Observation 2 on *co-GE*.

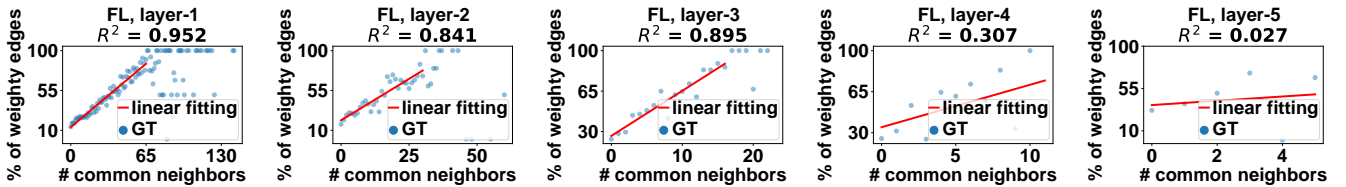Figure 21: The full results w.r.t Observation 2 on *OF*.

Figure 22: The full results w.r.t Observation 2 on *FL*.

1.3 Observation 3: a power law across layers

In Figures 23 to 33, for each dataset, we plot (a) the point $(f_{overall;i}, f_{0;i})$ for each $1 \leq i \leq 10$ [1] in the log-log scale and (b) the power-law fitting line, which is linear in the log-log scale. We include the formula and the R^2 value of each power-law fitting line.
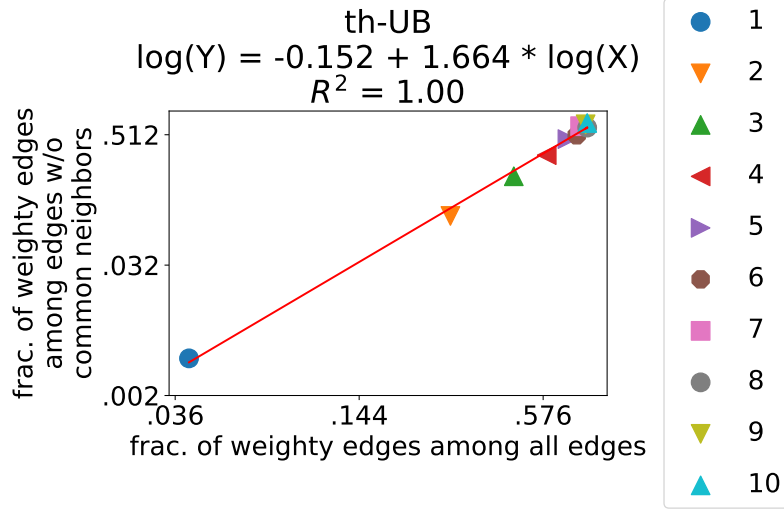

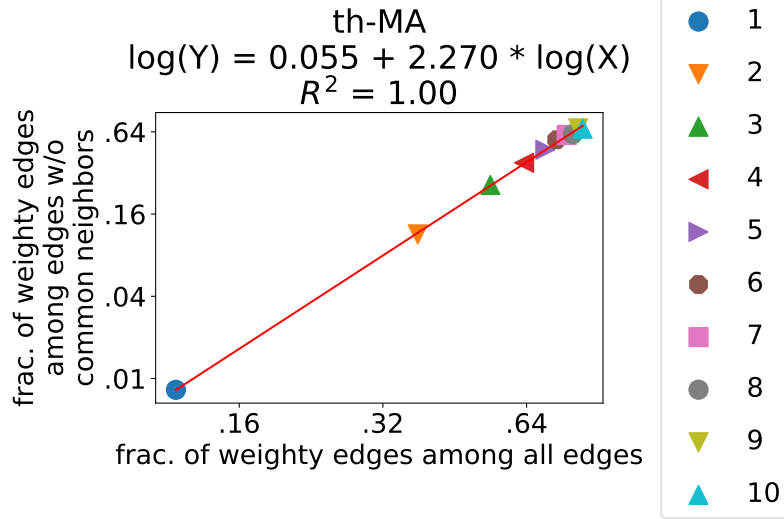Figure 23: The full results w.r.t Observation 3 on *th-UB*.

Figure 24: The full results w.r.t Observation 3 on *th-MA*.

---

[1] We only include the first four layers of FL since the layer-5 is too sparse and small and we skip the first layer of OF since the corresponding point is an outlier.
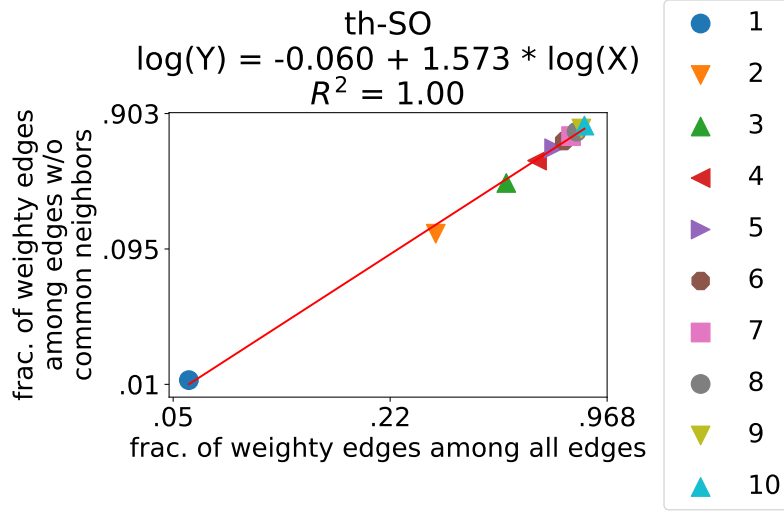
Figure 25: The full results w.r.t Observation 3 on *th-SO*.
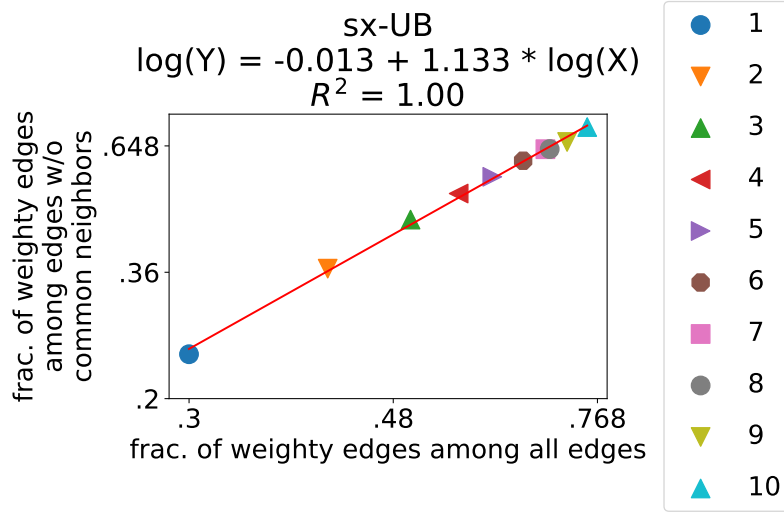

Figure 26: The full results w.r.t Observation 3 on *sx-UB*.
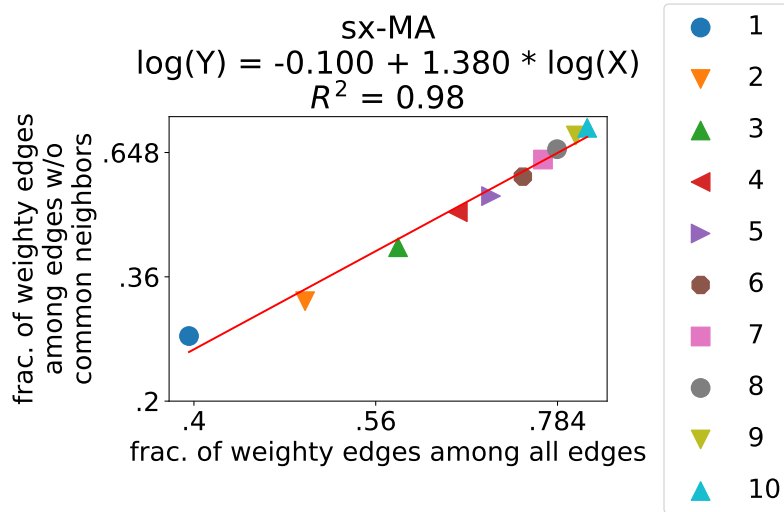

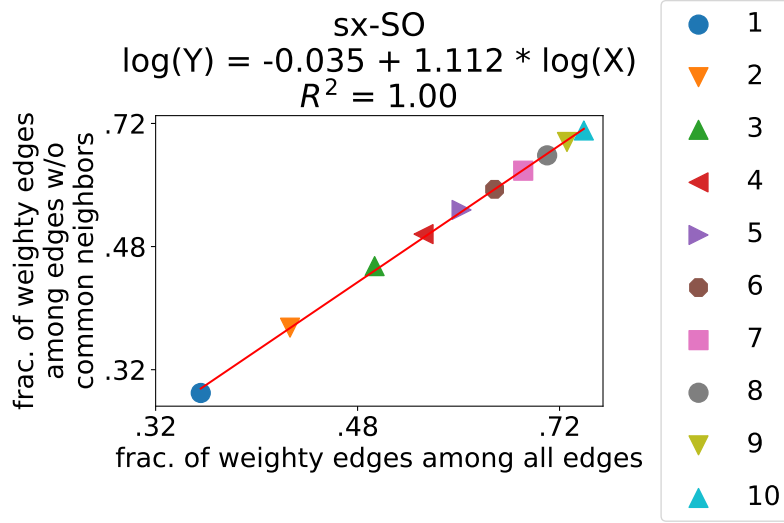Figure 27: The full results w.r.t Observation 3 on *sx-MA*.

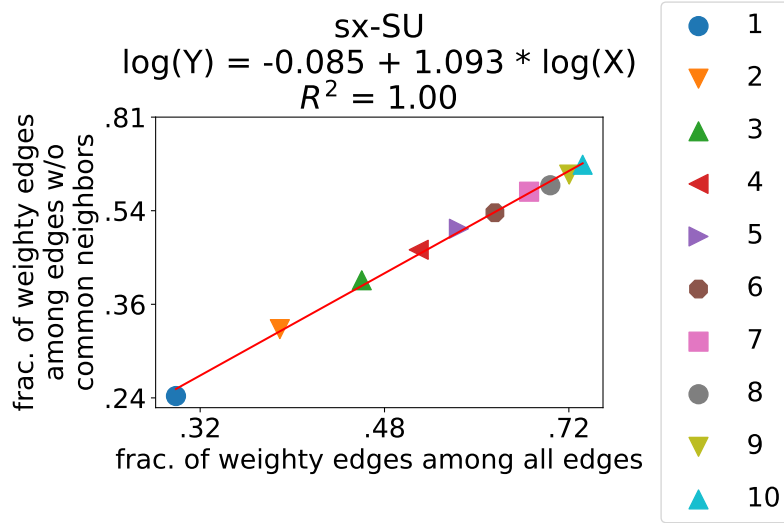Figure 28: The full results w.r.t Observation 3 on *sx-SO*.

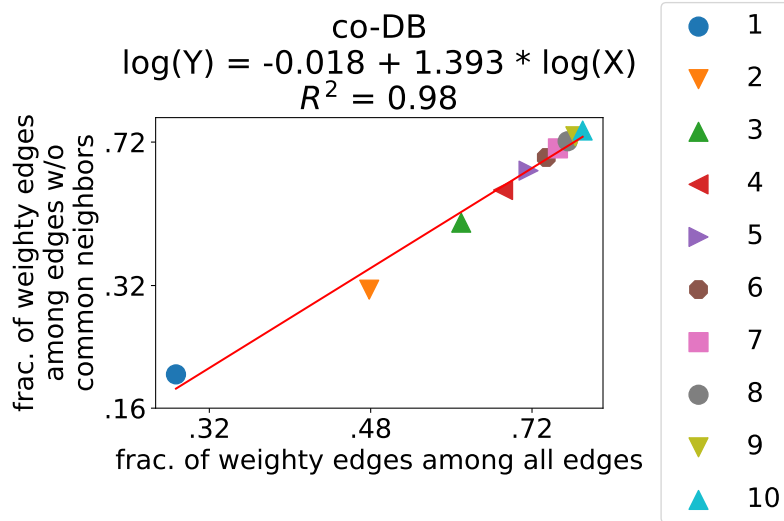Figure 29: The full results w.r.t Observation 3 on *sx-SU*.

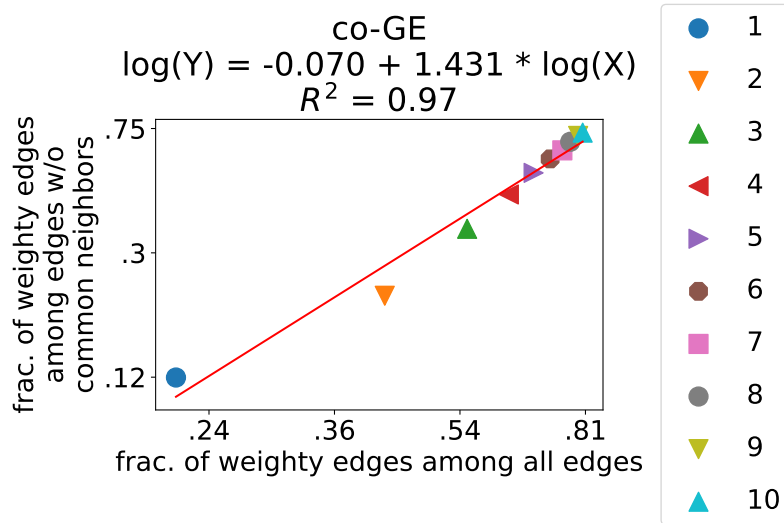Figure 30: The full results w.r.t Observation 3 on *co-DB*.

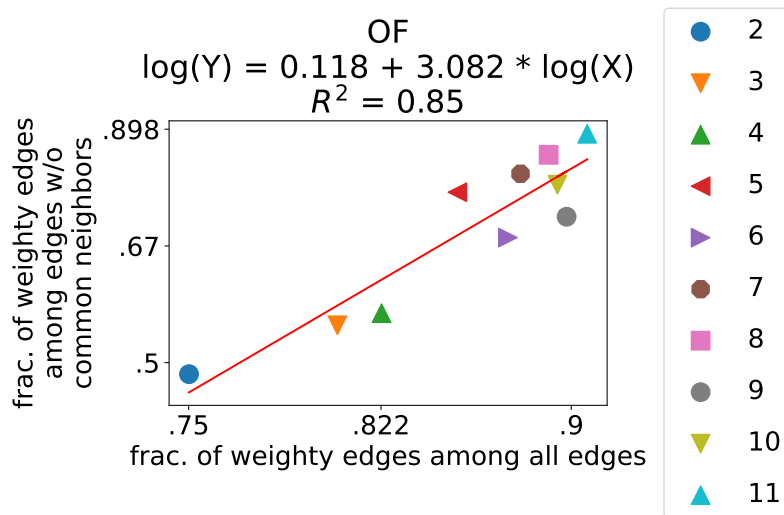Figure 31: The full results w.r.t Observation 3 on *co-GE*.
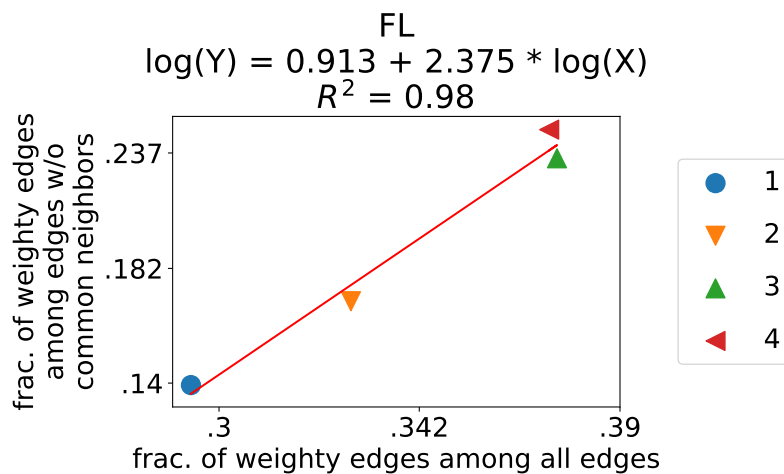

Figure 32: The full results w.r.t Observation 3 on *OF*.

Figure 33: The full results w.r.t Observation 3 on *FL*.